

Effects of Expandable Graphite and Dimethyl Methylphosphonate on Mechanical, Thermal, and Flame-Retardant Properties of Flexible Polyurethane Foams

Cheng-Qun Wang, Feng-Yan Ge, Jie Sun, Zai-Sheng Cai

Key Laboratory of Science and Technology of Eco-Textile, Ministry of Education, Donghua University, Shanghai 201620, People's Republic of China

Correspondence to: Z.-S. Cai (E-mail: zshcai@dhu.edu.cn)

ABSTRACT: Expandable graphite (EG) and dimethyl methylphosphonate (DMMP) were added to polyurethane to form flame-retardant high-resilience flexible polyurethane foam (FPUF) in one-step. The effects of EG and DMMP on cell morphology, mechanical properties, dynamic mechanical properties, thermal degradation, and flame-retardant properties of FPUF were studied. The results indicated that adding proper amount EG or/and DMMP would not seriously damage cell morphology and mechanical properties. Dynamic mechanical analysis (DMA) demonstrated that there were two $\tan \delta$ peaks attributed to soft and hard segment separately and 15 pbw EG or/and 15 pbw DMMP could enhance damping property of FPUF. Thermogravimetric analysis–Fourier transform infrared spectroscopy (TGA–FTIR) results indicated that 15 pbw EG or 15 pbw DMMP could improve the thermal stability of the second degradation step but there were no synergistic effect between the two. DMMP made FPUF composites produce more toxic gases such as CO, however, EG displayed an opposite effect. Both EG and DMMP could effectively improve the flame retardant properties of FPUF, and there was synergistic effect between the two. © 2013 Wiley Periodicals, Inc. *J. Appl. Polym. Sci.* 130: 916–926, 2013

KEYWORDS: degradation; flame retardance; foams; polyurethanes; composites

Received 7 December 2012; accepted 28 February 2013; published online 11 April 2013

DOI: 10.1002/app.39252

INTRODUCTION

Flexible polyurethane foams (FPUF) are primarily used for cushioning material with application in furniture, automobiles. FPUF readily ignites and burns rapidly with a high rate of heat release and evolution of smoke and toxic gases. More attention has been paying to improve flame-retardant properties of FPUF due to more strict standards being developed in traffic safety regulation.

The flammability is minimized by using different flame retardant additives based on halogen, phosphorus, nitrogen, boron, silicon, etc. They can take flame retardant effects either on the basis of condense-phase or gas-phase mechanism. Many kinds of flame retardants emanate toxic gases along with smoke during combustion especially halogenated compounds. Therefore, we need the flame retardant which can hardly pollute the environment. In recent years, many new nanofillers were being used as flame retardant, such as organo-modified montmorillonite (OMMT),¹ polyhedral oligomeric silsesquioxane (POSS),² carbon nanotubes (CNTs),³ etc. These new nanofillers can take effect on the basis of suspending heat swap mechanism, so their efficiency maybe is not very good.

Now expandable graphite (EG) is a new kind of physical intumescent flame retardant, and it is not only of high efficiency but also friendly to environment. EG is an intercalated graphite compound in which sulfuric acid has been inserted between the carbon layers of graphite. When graphite is heated to temperatures approximately 220°C, it can immediately react with sulfuric acid to generate CO₂, SO₂, and H₂O which can readily dilute oxygen. These gases make the graphite layers expand instantly to several 100 times, generating a dense char layer. This char layer acts as a physical barrier preventing the underlying material from the action of heat flux, and at the same time, limits the diffusion of combustible volatile products towards the flame and oxygen towards the polymer. EG is very suitable for polyurethane foams, because it not only can effectively improve its flame retardant properties but also hardly break the balance between gel reaction and blow reaction. Modesti et al.⁴ studied the flame-retardant properties of RPUF filled with expandable graphite (EG), ammonium polyphosphate (APP) or melamine cyanurate (MC), and concluded that the heat release rate of EG/RPUF was the lowest and limited oxygen index (LOI) value of EG/RPUF was the highest in the three. Thirumal et al.⁵ found that RPUF filled with the higher particle size EG showed

better mechanical properties and fire-retardant properties than the RPUF filled with the lower particle size EG. Li et al.^{6–12} found that EG not only can coordinate with other kind of flame-retardants producing synergistic effect but also possesses better flame-retardant ability after encapsulated with a layer of poly (methyl methacrylate). Bashirzadeh and Gharehbaghi¹³ concluded that EG performance in flame retardant, heat release, mass loss, and smoke generation was ideal. However, there is no more detailed report on the mechanical, pyrolysis, and flame-retardant behaviors of EG-filled FPUF system.

EG could also deteriorate the mechanical properties of FPUF because of the poor interfacial adhesion between EG particles and the polymer matrix if it was filled too much EG aiming to achieve higher standards flame retardant EG/FPUF. The total amount of flame retardant should decrease to get the same flame retardant level when two kinds of flame retardants were added together in FPUF. Among commercially available phosphonates, dimethyl methylphosphonate (DMMP) seems a suitable choice for FPUF with the advantages of low viscosity (1.75 mPa·s), low toxicity, high phosphate content (25%), high chemical stability, low melting point (-50°C), and high boiling point (180°C). Therefore, not only its flame retardant efficiency is outstanding but also it can hardly break the balance between gel reaction and blow reaction.

Modesti et al.^{14,15} studied the flame retardant properties of RPUF filled with EG and triethylphosphate (TEP) and concluded that the LOI value of EG-TEP/RPUF was improved greatly and EG-TEP could decrease heat release rate apparently. The phosphorus content of TEP is about 17% which is much smaller than that of DMMP, so it is more feasible for DMMP to make the combustible material become flame retardant.¹⁶ Chen et al.¹⁷ investigated the flame retardant, thermal stable, and mechanical properties of polyurethane foams (PUFs) filled with several halogen-free flame retardants and concluded that PUFs filled with DMMP had better flame retardancy compared with TEP and DMMP degraded at a low temperature to form several phosphorated acids which accelerated the formation of char layer. However, few reports have been published about the synergistic effect of DMMP and EG in FPUF. In this study, EG and DMMP were introduced to FPUF by cast molding. The flammability of the materials was evaluated by FMVSS 302 tests and LOI tests. The dynamic mechanical properties and thermal degradation behavior were investigated using DMA and TGA-FTIR separately.

EXPERIMENTAL

Materials

The raw materials used in this study include the following:

1. Polyether polyol, GEP-330N, obtained from Dongda Chemical Co. (Shandong, China). Main properties: functionality, 3.0; typical hydroxyl number, $32 \sim 36$ mg potassium hydroxide (KOH) equiv/g; primary hydroxyl radical, $\geq 70\%$; viscosity (25°C), $800 \sim 1000$ mPa·s; number average molecular weight, $M_n \approx 5000$ g/mol.
2. Polyether polyol, GOP36/28, prepared by acrylonitrile and phenylethylene, obtained from Dongda Chemical Co. (Shandong, China). Main properties: functionality, 3.0;

typical hydroxyl number, $25 \sim 29$ mg potassium hydroxide (KOH) equiv/g; viscosity (25°C) ≤ 3500 mPa·s, number average molecular weight, $M_n \approx 6000$ g/mol.

3. Diethanolamine, crosslink catalyst, provided by Shanghai Chemical Reagent Co. (Shanghai, China).
4. Y-10366, silicone oil, a kind of surfactant for polyurethane high resilience flexible foam, provided by American Momentive Co.
5. Distilled water, blowing agent.
6. A-33, catalyst for the gel and blow reaction, a dipropylene glycol solution of triethylenediamine (mass fraction of 33%), provided by Shanghai Chemical Reagent Co. (Shanghai, China).
7. A-1, equilibrium catalyst, provided by Daoning Chemical Co. (Foshan, China).
8. Isocyanate (TDI80), a 80/20 mixture of 2,4- and 2,6-toluene diisocyanate, provided by Germany Basf (China) Co., -NCO content, 48 wt %.
9. Isocyanate (PMDI), 44V20L, Bayer Co. (German). Main properties: viscosity (25°C), $150 \sim 250$ mPa·s; -NCO content, 31 wt %.
10. EG, flame retardants, obtained from Fuyouqin trade Co. (Shanghai, China). Main properties: ash 1.0%; moisture 1.0%; volatile, 15%; pH value 3.5; average particle diameter $180 \mu\text{m}$; expansion rate 50 mL/g.
11. Dimethyl methylphosphonate, obtained from Zhenxing Chemical Co. (Hebei, China). Main properties: phosphorous content, 25 wt %, density (25°C), 1.16 g/cm^3 , viscosity (25°C) 17.5 mPa·s.

Foam Composites Preparation

A one-shot, free-rise method was used to prepare neat FPUF by a cast mold whose internal surfaces were painted with a stripping agent. The stripping agent can make cohesive force between sample surface and mold surface decrease sharply, then samples can be taken out smoothly and entirely. All components except EG, DMMP, and isocyanate were mixed and stirred with an electric stirrer until a uniform mixture was obtained. Isocyanate was then quickly added into the suspension. After high speed stirring at 1400 rpm for about 4 s, the mixture was poured quickly into the cast mold completely covered with a lid. When frothy bubbles formed, the mold was put into an oven and heated for 2 h at 55°C . The foam was then taken out from the mold. Test samples with their coats removed were machined in accordance to the test standard. EG or/and DMMP filled FPUF were prepared by the same way, and they were mixed with other components before adding isocyanate.

In this study, the density of foam was controlled to approximately $(55 \pm 0.5) \text{ kg} \cdot \text{m}^{-3}$ by varying the dosage of distilled water. The molar ratio of NCO to OH was 1.20; the weight ratio of polyol to isocyanate was 100 : 38 and the weight ratio of TDI80 to PMDI was 3 : 2. Formulations of pure FPUF and flame-retardant FPUF are shown in Table I. When 15 pbw EG or 15 pbw DMMP was added into FPUF, the sample name was abbreviated as 15 pbw EG/FPUF or 15 pbw DMMP/FPUF.

Table I. Parameters of Flame-Retardant FPUF

Materials	FPUF	EG/FPUF	DMMP/FPUF	(EG+DMMP)/FPUF
Polyether polyol 330N (pbw ^a)	50	50	50	50
Polymer polyol 3628 (pbw)	50	50	50	50
Catalyst A-1 (pbw)	0.1	0.1	0.1	0.1
Catalyst A-33 (pbw)	1.5	1.5	1.5	1.5
Diethanolamine (pbw)	2.5	2.5	2.5	2.5
Silicone Y-10366 (pbw)	1.7	1.7	1.7	1.7
Distilled water (pbw)	2.75	2.75 ~ 3	2.5 ~ 2.75	2.5 ~ 3
Expandable graphite (pbw)	-	5 ~ 15	-	5 ~ 15
Dimethylmethylphosphate (pbw)	-	-	5 ~ 15	5 ~ 15
Isocyanate (TDI 80) (pbw)	23	23	23	23
Isocyanate (PMDI) (pbw)	15	15	15	15

^apbw: part by weight.

Characterization

Scanning Electron Microscopy (SEM). The original and burned samples were fractured at room temperature and coated with gold before being investigated under a scanning electron microscope. The fracture surfaces of the samples were observed with a JSM-5600LV (JEOL Japan) SEM with an accelerating voltage of 10 kV.

Tensile and Compression Test. Tensile measurements were performed with a H5K-S all-purpose material test instrument (Hounsfield Co., UK) in accordance to the DIN 53455 at a speed rate of 50 mm/min. Compression set test was carried out with a parallel plate clam on columns of size 50 × 50 × 50 mm³ according to GB/T6669-1986 at 70°C for 22 h.

Dynamic Mechanical Analysis. Dynamic mechanical analysis (DMA) machine used to measure the strain mode was a Q800 DMA instrument (TA) with a heating rate 3°C/min from -80 to 180°C and a vibration frequency of 1 Hz. The sample size was 15 × 10 × 5 mm³.

Horizontal Burning Test. Flame spread rate from a small flame source of FPUF was determined using Motor Vehicle Safety System no. 302 (FMVSS 302) which is shown in Table II. A horizontal burning instrument (Dalong Co., China) was used to test the horizontal burning classification. The specimens used in this test were processed into sheets of 250 × 102 × 13 mm³.

Limited Oxygen Index (LOI) Test. LOI was measured with a JF-3 oxygen index test instrument (Nanjing analysis instrument Co., China) on specimen sheets of 130 × 10 × 10 mm³ according to the test standard "oxygen index" test ASTM D 2863-97.

Thermogravimetric Analysis–Fourier Transform Infrared Spectroscopy. TGA was carried out at 20°C/min under nitrogen (flow rate: 20 mL/min) with a thermogravimetric analyzer (Netzsch TG 209 F1 Iris). In each test, the mass of the test sample was 5 mg, and the samples were heated from 25 to 800°C. There was a guide tube heated to 210°C which connected thermogravimetric analyzer and FTIR spectrometer (Nicolet 8700). Pyrolysis gases from the samples in the thermogravimetric analyzer were blown to the FTIR spectrometer with the guide by

nitrogen. About 32 scans within the range of 4000–400 cm⁻¹ were done for each sample with a resolution of 8 cm⁻¹.

RESULTS AND DISCUSSION

Morphology of FPUF Composites

Figure 1 shows the SEM micrographs of the FPUF, 15 pbw EG-or/and 15 pbw DMMP-filled FPUF. For pure FPUF shown in Figure 1(A), the shape of the cells is regular, with no collapse or collision in the cell system being observed. Most cells are open, and some are closed by thin films. In addition, not only are the diameters of the cells approximately uniform but also the cell walls are integrated. In contrast, Figure 1(B) demonstrates that 15 pbw EG made the diameter of the cells uneven a little because solid EG caused great resistance while foaming, and

Table II. FMVSS 302 Classification

FMVSS 302	Interpretation
Non-combustible DNI (does not ignite)	The material does not burn or self goes out when the flame front is no more in contact with the Bunsen burner.
Auto-extinguishable SE (self-extinguishing)	The material burns and the combustion stops before the flame gets over the first reference mark.
SE/NBR (self-extinguishing/ no burn rate)	The material burns and stops burning less than 60 s after the beginning of the time keeping and has not burnt over a distance superior to 51mm from the reference mark.
SE/B (self-extinguishing with burn rate)	The material burns and the flame self-extinguishes between the two reference marks (previous case excluded).
Combustible B (burn rate)	The combustion crosses the second reference mark.

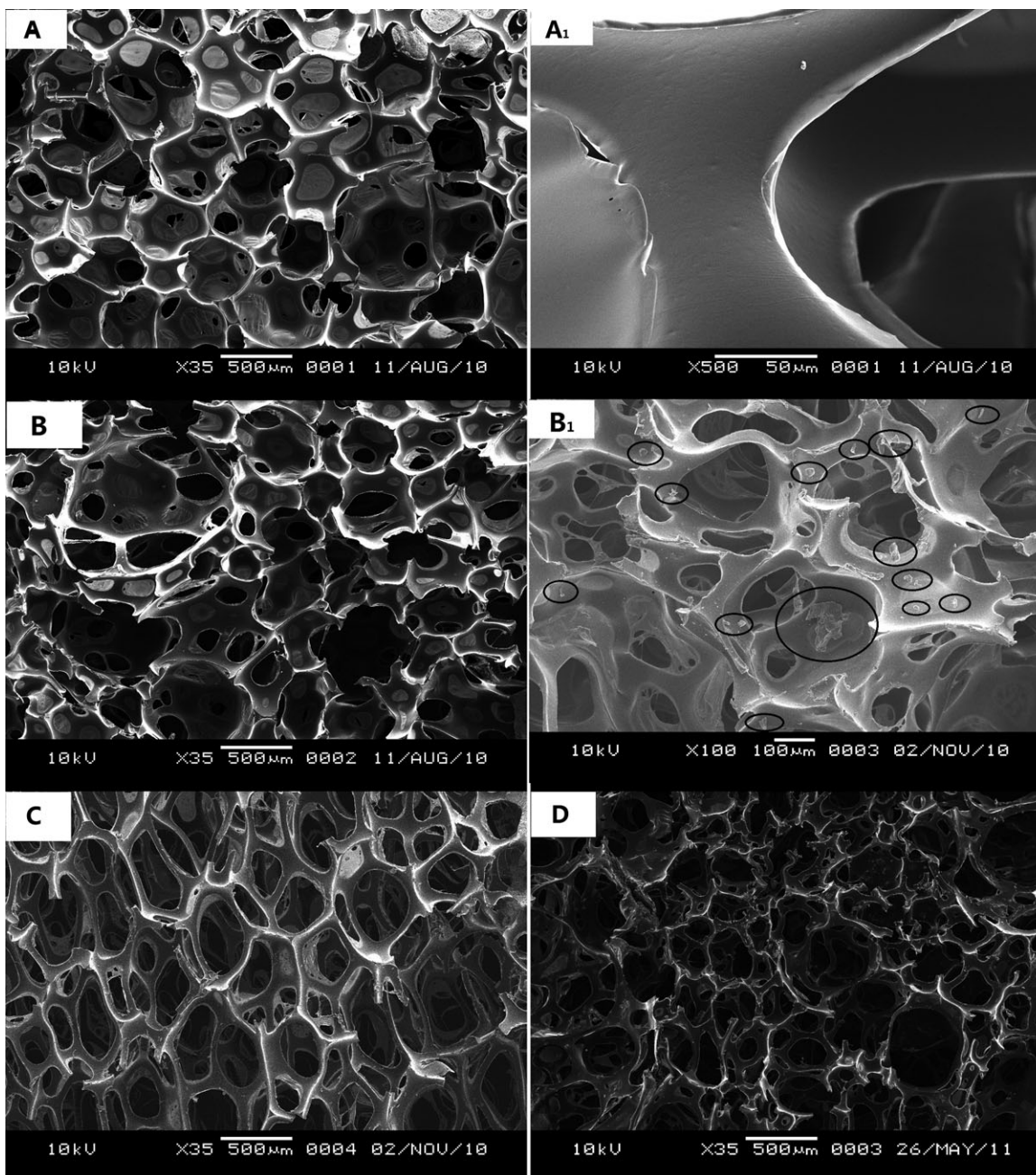


Figure 1. SEM micrographs of the FPUF and flame-retardants filled FPUF. (A) FPUF ($\times 35$); (A₁) FPUF ($\times 500$); (B) 15 pbw EG/FPUF ($\times 35$); (B₁) 15 pbw EG/FPUF ($\times 100$); (C) 15 pbw DMMP/FPUF ($\times 35$); (D) (15 pbw EG + 15 pbw DMMP)/FPUF ($\times 35$).

Table III. Mechanical Properties of the FPUF with EG and DMMP as Flame Retardants

	Tensile strength (kPa)	Tensile rupture elongation (%)	50% compress set (%)	Number of cells (cm ⁻¹)	
				Horizontal orientation	Vertical orientation
FPUF	104.0 ± 4.8	112.6 ± 5.7	7.5 ± 0.5	23.3 ± 2.1	25.0 ± 1.7
15 pbw EG/FPUF	98.0 ± 5.6	74.8 ± 6.2	8.4 ± 0.7	20.3 ± 2.2	22.5 ± 2.5
15 pbw DMMP /FPUF	95.5 ± 3.7	118.5 ± 4.8	9.7 ± 0.4	23.3 ± 1.6	17.5 ± 1.2
(15 pbw EG + 15 pbw DMMP)/FPUF	95.4 ± 6.3	85.8 ± 6.8	9.1 ± 0.8	26.7 ± 2.8	22.5 ± 2.6

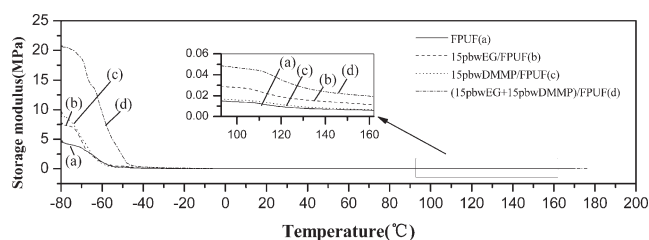


Figure 2. Effect of the flame-retardants on the storage modulus of the FPUF composite.

also —OH group of EG surface could react with —NCO of TDI or MDI. Comparing Figure 1 (A₁) with (B₁), the EG particles mainly locate themselves on the cell walls. Although the cell walls were transformed at a certain extent, EG hardly destroyed the integrity of cells because it did not span cells and this is due to EG size still being smaller than the cell size. According to Figure 1(D), although the total content of EG and DMMP was very high, the cell structure of (15 pbw EG + 15 pbw DMMP)/FPUF still accorded with standard, probably due to DMMP reduce the viscosity of the mixture, leading to more uniform dispersion of EG.

Tensile and Compression Properties

Tensile strength, elongation, 50% compress set, and number of cells of the FPUF, EG, and DMMP-filled FPUF are listed in Table III. In Table III, both 15 pbw EG and 15 pbw DMMP made the value of tensile strength decrease and 50% compress set increase. This shows that EG or DMMP leads to worsening of mechanical property. The reason may be due to the poor compatibility between EG or DMMP and the polymer matrix, but not remarkable. The tensile rupture elongation of 15 pbw DMMP/FPUF increased but that of 15 pbw EG/FPUF decreased. These resultant effects of DMMP on FPUF can be explained as follows: The plasticizing effect of DMMP made the distance between molecular chains increase thereby weakening the H-bond forces in the hard and soft segments, hence PU molecular chains tended to slide over one another instead of being ruptured.¹⁸ Figure 1(C) shows how DMMP made all the cells open completely and this can be attributed to the lower viscosity additives which made flowing easy leading to weaker resistance while foaming. For the same reason, it was easier for the cells to elongate along foaming direction. This is shown in Table III,

where the number of cells in horizontal orientation is more than those in vertical orientation.

Dynamic Mechanical Properties

Since high-resilience flexible foams are often used as a seat material in aircraft and other vehicles, its damping performance is of high significance. The DMA is a widely used technique for examining the viscoelastic behavior of PU foams, which can give information about their viscoelastic properties like the energy dissipation of soft and hard materials.^{19,20} When an interface between flame retardant and a substrate layer is formed, the dynamic mechanical properties can be used to reflect the formation of this interface. The storage modulus (E'), loss modulus (E''), and loss factor ($\tan \delta$) curves obtained from the DMA measurement of FPUF composite are shown in Figures 2–4.

Figure 2 represents the variations of E' as a function of the temperature of FPUF, 15 pbw EG/FPUF, 15 pbw DMMP/FPUF, and (15 pbw EG + 15 pbw DMMP)/FPUF obtained from DMA measurement. From -80°C to -40°C , the E' of the four samples decreased sharply, indicating that the macromolecular chain was undergoing a reversible sliding. Within the range of -80 to -65°C , the E' of EG- or DMMP-FPUF was higher than that of pure FPUF, indicating that both the two additives improve stiffness of FPUF. The thermal motion of molecular chains was restricted by EG located on struts or knots of FPUF cells or partly embedded in the struts. Similarly, solidified DMMP were evenly distributed among the macromolecular chains which necessarily restricted the molecular chain movement, thus leading to a higher E' than that of EG. In the range of -80 to -50°C , it can be easily evaluated that the E' values of (15 pbw EG + 15 pbw DMMP)/FPUF were higher than the sum of the two E' values of 15 pbw EG/FPUF and 15 pbw DMMP/FPUF at the same temperature, indicating that EG and DMMP had a collaborative effect on enhancing stiffness of FPUF. The reason for the result is probably that the melting point of DMMP was -50°C , so it appeared solid state in the range of -80 to -50°C , leading EG tightly frozen on the cell wall because there was certainly a little DMMP on the cell wall or EG surface.

The loss modulus (E'') of FPUF, 15 pbw EG/FPUF, 15 pbw DMMP/FPUF, and (15 pbw EG + 15 pbw DMMP)/FPUF are shown in Figure 3. With molecular chains movement, greater friction was generated between macromolecular chains and EG particles or frozen DMMP in the range of -80 to -50°C , which

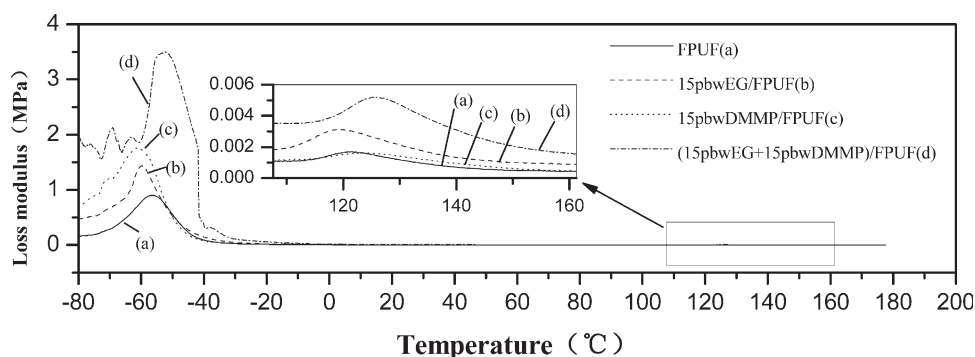


Figure 3. Effect of the flame retardants on the loss modulus of the FPUF composite.

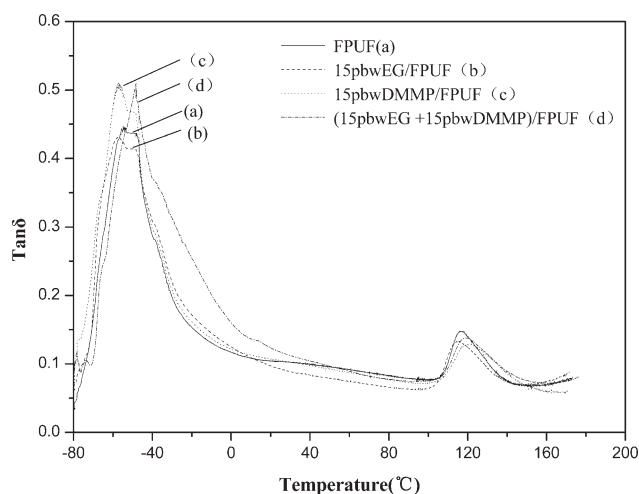


Figure 4. Effect of the flame retardants on the $\tan \delta$ of the FPUF composite.

led to higher E'' value. EG particles are so large that most of them are found on foam walls. In contrast, solidified DMMP evenly and extensively distributes itself among polyurethane molecular chains, resulting in more friction than EG.

Figure 4 shows the loss tangent ($\tan \delta$) versus the temperature for the pure FPUF and FPUF with flame retardants, and Table IV shows parameters for $\tan \delta$ curves. It can be seen that there are two peaks on each curve, which represents glass-transition temperatures (T_g) for soft segments (SSs) and hard segments (HSs) of polyurethane, respectively. However, we cannot see one transition, at around 120 °C, attributed to HSs in the storage modulus-temperature curve and the loss modulus-temperature curve. This is because the values are too low to display, compared to that of SSs. So we can see the peak at around 120 °C in partial enlarged figure of Figures 2 and 3.

Table IV shows that the $\tan \delta_{\max}$ of 15 pbw EG/FPUF is slightly lower than that of FPUF, while the $\tan \delta_{\max}$ of 15 pbw DMMP/FPUF or (15 pbw EG + 15 pbw DMMP)/FPUF is higher than that of FPUF, indicating that EG made $\tan \delta_{\max}$ decrease and DMMP made $\tan \delta_{\max}$ increase. Lower $\tan \delta$ indicates that the foam formulations have a more elastic nature than viscous nature, and vice versa. This means that EG decreased the crosslink degree of FPUF, and further improved elastic nature. In contrast, DMMP made viscous nature of FPUF composites to be

enhanced. Generally, the material whose $\tan \delta$ value is beyond 0.3 can be considered to have a damping effect. EG or DMMP made the temperature range of $\tan \delta > 0.3$ increase slightly, and addition of EG and DMMP together increased the range significantly. The increase of the temperature range for damping effect is due to the restriction of molecular motion by incorporation of additives. On the other hand, for HSs of FPUF, $\tan \delta_{\max}$ decreased slightly after adding EG or DMMP; while the peak areas changed slightly. The temperature of $\tan \delta_{\max}$ represents the glass transition temperature (T_g). From Figure 4 and Table IV, EG or DMMP did not change the T_g significantly, which may be due to fewer reactions between additive flame retardants and polyurethane resin.

Flammability Properties

Compared to other kinds of plastics, FPUF has lots of large and opened pores leading to its low density. Therefore, in the vertical burning test, FPUF burned fast and completely even when filled with 15 pbw EG or DMMP. Consequently, it was found suitable to be classified by the horizontal burning test.¹²

Table V shows flammability results of FPUF composite analyzed by horizontal burning tests—FMVSS 302 testing which is very suitable for automotive seat foam in America. Pure FPUF itself should have a combustible level, but from Table V, it is SE/B level, because the burning flame was taken away by dripping. However, the burning rate could still reach 91 mm·min⁻¹. After adding 15 pbw EG or DMMP, the burning test was still SE rating, and when the total content of the two additions was fixed at 5 pbw and their ratios changed, the flame-retardant level of 5 pbw (EG + DMMP)/FPUF was also SE/NBR level. In case of fire, FPUF melts to a liquid. Instead of forming a droplet, liquid PU covers a large volume of the expanded graphite, which causes an increased surface with an increase in mass flux maybe resulting in a little higher burning velocity.²¹ At the same time, the droplet is restrained because of absorption of large volume of expanded graphite. In contrast, DMMP accelerated the droplet because it increased the fluidity of the system, as shown in Table V.

Figure 5 shows the results of the LOI burning tests of DMMP/FPUF and EG/FPUF. The LOI values increased with the increase of EG or DMMP content. When EG or DMMP content is 15 pbw, the LOI values increase to 23 and 24.5 vol %, respectively. At the same content, LOI value of DMMP/FPUF is higher than that of EG/FPUF. One of the reasons for this is that DMMP has higher phosphorus content.

Table IV. Parameters of Loss Tangent ($\tan \delta$) Versus Temperature Curves of Samples

	FPUF		15 pbw EG /FPUF		15 pbw DMMP/FPUF		(15 pbw EG + 15 pbw DMMP)/FPUF	
	SSs	HSs	SSs	HSs	SSs	HSs	SSs	HSs
$\tan \delta_{\max}$	0.44	0.15	0.43	0.13	0.51	0.13	0.51	0.14
Temperature of $\tan \delta_{\max}$ (°C)	-52	119	-50	117	-55	122	-45	120
Temperature range of $\tan \delta_{\max} > 0.3$ (°C)	-61 to -40	-	-65 to -38	-	-66 to -40	-	-59 to -28	-
Δt (°C)	21	-	27	-	26	-	31	-

Table V. Horizontal Burning Tests Formulations of FPUF Filled with EG or/and DMMP

No.	EG (pbw)	DMMP (pbw)	Dripping	FMVSS 302 classification
1	0	0	Y	SE/B
2	5	0	N	SE/NBR
3	10	0	N	SE
4	15	0	N	SE
5	0	5	Y	SE
6	0	10	Y	SE
7	0	15	Y	SE
8	1	4	Y	SE/NBR
9	2.5	2.5	Y	SE/NBR
10	4	1	N	SE/NBR

LOI test is a useful means to verify if there is synergistic effect between the two flame retardants. The total content of the two additions was fixed (15 pbw) and their ratios changed. The LOI values are shown in Figure 6. It can be seen that the LOI curve lies above the critical curve (broken line), which indicates that there is synergistic effect between the two flame retardants. When the EG: DMMP ratio was 5 : 10, the vertical distance between the point and the critical curve reached maximum, indicating that it is the best ratio for EG and DMMP in FPUF. The reason for synergistic effect was because they can both take effect in condense-phase, and DMMP also can take effect in gas-phase.²²

Thermal Degradation Analysis

Figures 7 and 8 show the thermogravimetric analysis (TGA) and derivative thermogravimetric (DTG) curves of FPUF, 15 pbw EG/FPUF, 15 pbw DMMP/FPUF, and (15 pbw EG + 15 pbw DMMP)/FPUF under a flow of nitrogen, respectively. Table VI shows the parameters of TGA and DTG curves, including the degradation temperature range (T_{1stage} , T_{2stage}), the maximum degradation temperature (T_{1max} , T_{2max}), the maximum

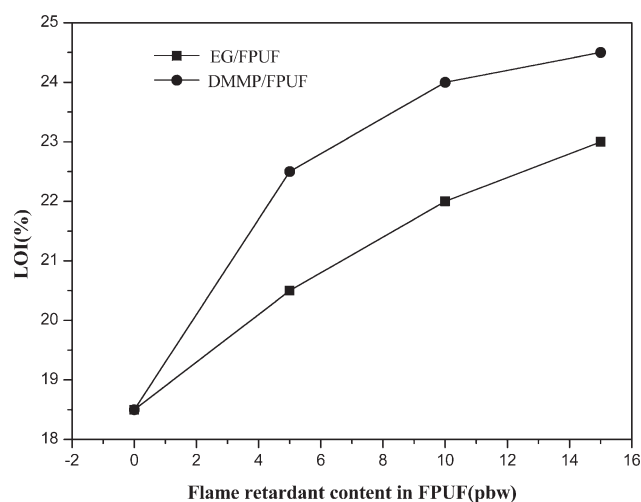
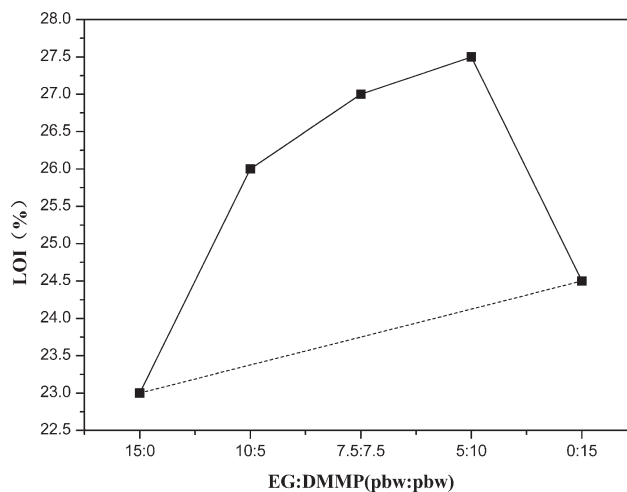
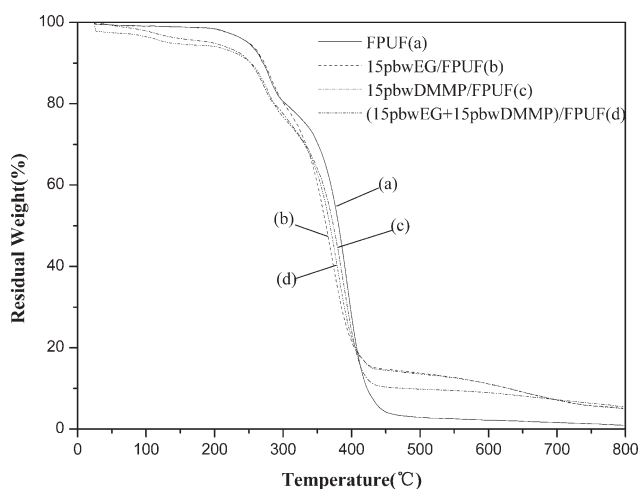
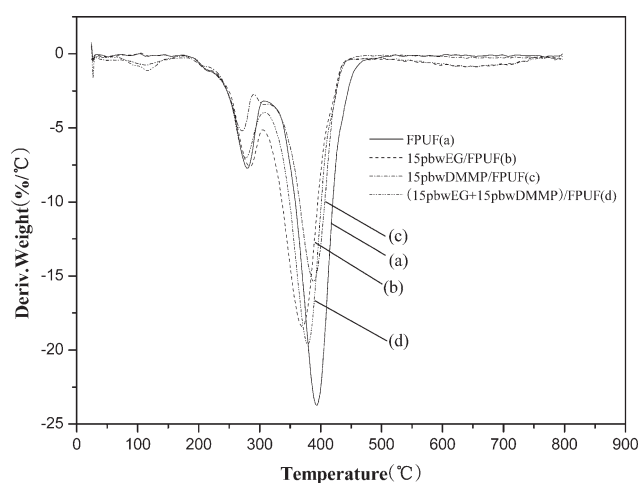
**Figure 5.** LOI curves of EG/FPUF and DMMP/FPUF.**Figure 6.** Synergistic effect of EG/DMMP systems on the LOI values.**Figure 7.** TG curves of pure FPUF and flame-retardants filled FPUF.**Figure 8.** DTG curves of pure FPUF and flame retardants filled FPUF.

Table VI. Effect of EG and DMMP on the Degradation Temperature and Velocity and Residual Mass of FPUF

Sample	T_{stage} ($^{\circ}\text{C}$)		T_{max} ($^{\circ}\text{C}$), $V_{\text{max}}^{\text{a}}$ (%/ $^{\circ}\text{C}$)		Residual mass (%)
	$T_{1\text{stage}}$	$T_{2\text{stage}}$	$T_{1\text{max}}, V_{1\text{max}}$	$T_{2\text{max}}, V_{2\text{max}}$	
PUF	240~310	330~460	279, 7.7	394, 23.8	0.9
15 pbw EG/FPUF	240~310	325~440	284, 7.6	369, 18.4	5.2
15 pbw DMMP/FPUF	240~295	330~440	272, 5.2	390, 15.4	5.5
(15 pbw EG + 15 pbw DMMP)/FPUF	240~310	325~440	276, 7.0	378, 19.6	5.0

^a V_{max} : maximum decompose velocity.

degradation velocity ($V_{1\text{max}}$, $V_{2\text{max}}$) and the residual of mass at 800°C .

In Figures 7 and 8, all samples exhibited two main degradation stages. The first mass loss can be attributed to the degradation of HSs because of the relatively low thermal stability of the urethane group. In this stage, isocyanate and carbon dioxide evaporated. The second mass loss was due to SSs decomposition. In this stage, there are many kinds of gases released, such as carbon monoxide, carbon dioxide, and so on.²³ In the range of 410 – 650°C , the residual mass of 15 pbw EG/FPUF or (15 pbw EG + 15 pbw DMMP)/FPUF was higher than that of 15 pbw DMMP/FPUF, but the residual masses of the three were the same, but higher than that of FPUF at 800°C .

The effect of EG on the first degradation step of FPUF was less, because expansion of EG and the first degradation step of FPUF occurred simultaneously. The parameters ($T_{2\text{stage}}$, $T_{2\text{max}}$, $V_{2\text{max}}$) of the second degradation steps of FPUF and 15 pbw EG/FPUF were different. On one hand, the $T_{2\text{stage}}$ range of 15 pbw EG/FPUF was lower than that of FPUF, which was due to the decomposition of EG occurring earlier than the second decomposition step of FPUF. On the other hand, $V_{2\text{max}}$ reduced from $23.8\%/^{\circ}\text{C}$ to $18.4\%/^{\circ}\text{C}$ after addition EG, indicating that expanded carbon layer of EG acted as a heat insulator, reducing thermal degradation rate, and increasing thermal stability.

The effect of DMMP on the first and second thermal degradation steps were both evident. In the first place, DMMP was decomposed to phosphoric acid at about 180°C , which further degenerated to metaphosphoric acid and polymetaphosphoric acid. These products could act as a catalyst for urethane bond breaking,²⁴ so $T_{1\text{stage}}$ and $T_{1\text{max}}$ decreased slightly. Moreover, DMMP dehydrated to coke residue and the products covered FPUF substrate, which made thermal conductivity and decomposition rate decreased.

Comparing the curves of (15 pbw EG + 15 pbw DMMP)/FPUF and the other three samples, it can be seen that 15 pbw EG together with 15 pbw DMMP did not change the first step thermal degradation process, and its $T_{2\text{stage}}$ is similar to that of 15 pbw EG/FPUF and 15 pbw DMMP/FPUF. However, $T_{2\text{max}}$ is in between and $V_{2\text{max}}$ is greater than the two values. This indicates that there was no synergistic effect between EG and DMMP in thermal stability of FPUF. The reason may be that phosphoric acid covered large expanded graphite instead of hot-melt FPUF.²¹

Figure 9 shows 3D FTIR spectra for the gases produced from thermal degradation of FPUF composites. The absorption peaks

in the range 2700 – 3200 cm^{-1} can be attributed to the volatilization of aliphatic carbon group such as CH_3 - and $-\text{CH}_2$ -. The absorption peaks at 2359 and 669 cm^{-1} , which correspond to the evolution of carbon dioxide, appear in both the first and the second degradation steps. The absorption peaks at 2030 – 2220 cm^{-1} , which correspond to the evolution of carbon monoxide, mainly appear in the second degradation steps. The peaks at about 1100 and 1750 cm^{-1} can be attributed to the absorption of C-O radicals of ether and C=O radicals of aldehydes or ketones respectively. As can be seen in Figure 9(A), the CO or CO_2 yield always increased in pace with improvement of temperature for the reason of oxidative effect of molecule interior, and this situation displayed more serious when DMMP was added in FPUF in Figure 9(C,D). It is easily to understand that aldehydes or ketones, ether, and aliphatic compound mainly appeared during degradation process of FPUF in the range of 200 – 450°C , and DMMP made the yields of these products increase but EG seemingly decrease the yields in Figure 9(B).

Figure 10 shows the FTIR spectra of gases evolved from the four samples at 400°C . It can be seen that the big difference between 15 pbw EG/FPUF and the other three samples is that the absorption the peak of CO decrease apparently and the absorption peak of CO_2 increase. However, DMMP displayed an opposite effect due to DMMP functioned by transforming pyrolysis process of the foam.²⁵

Morphology of the Burned Char Layers of FPUF Composites

Figure 11 shows the overall regions from the unburned region to the burned region of FPUF, 15 pbw EG/FPUF, 15 pbw DMMP/FPUF and (15 pbw EG + 15 pbw DMMP)/FPUF after the horizontal burning test. From Figure 11(A), it can be seen that there was little residual char remaining. This was because the droplet was serious when FPUF was burning hence the bubble surface was directly exposed to burning flame, making it easy for heat to melt the foam thus the foam cells were out of shape.

DMMP is a good radical inhibitor by capturing the radicals $\text{H}\cdot$ and $\text{HO}\cdot$ in the flame zone hence it can weaken or terminate combustion chain branching reactions. Furthermore, H_3PO_4 can be decomposed further to produce the radicals $\text{PO}\cdot$ and $\text{PO}_2\cdot$, which can also capture $\text{H}\cdot$ and $\text{HO}\cdot$.²² Also, non-volatile phosphate layer acted as a protective layer of insulation, which covered the burning area and cut off heat transfer and oxygen

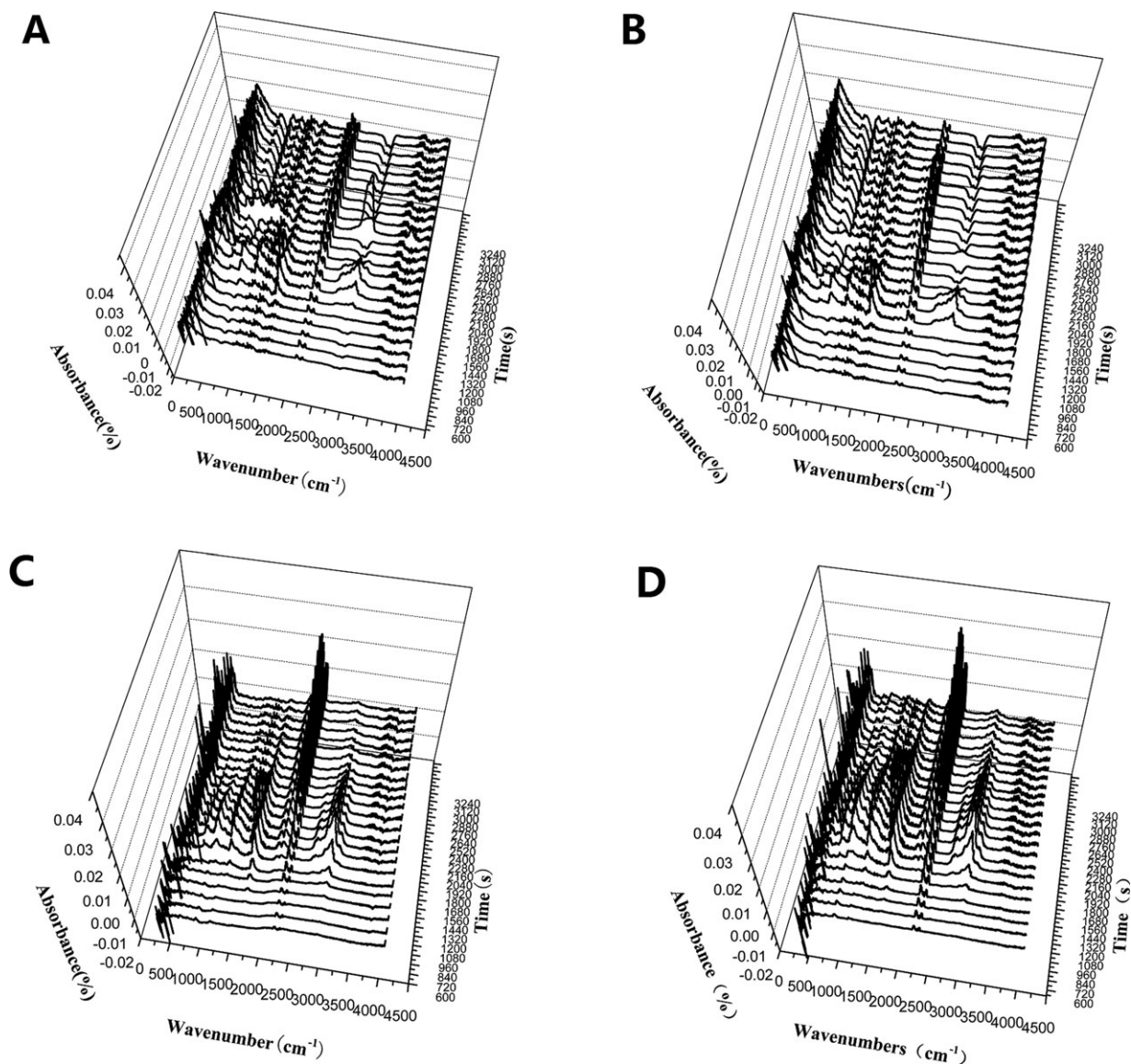


Figure 9. The FTIR spectra of FPUF filled with flame retardants at different time as test by TG-FTIR.

supply. However, as shown in Figure 11(C), there was only deformed foam without residual char because of droplet.

The expanded graphite covered the combustion point of the substrate surface. So it not only hindered the external heat to the polymer, but also limited the evaporation of combustible gas from the polymer. In Figure 11(B), there is a clear boundary between the inside layer and the burned outside char layer. Due to protection of expanded graphite, the internal foam cells next to expanded graphite were not thermally distortion. Expanded graphite is bulky and its surface is bumpy because of fracture and pore. This makes it possess a good absorption ability to inhibit the droplet.

Figure 11(D) shows a more compact “worm-like” char than Figure 11(B). The reason for this probably is that the products of DMMP/FPUF decomposition were so viscous that they increased bond force between the expanded graphite

layers. Thus the char layer should be more stable and larger, reducing the “fly ash” phenomenon. So this is the mainly reason of flame retardant synergistic effect between EG and DMMP.

CONCLUSIONS

Although EG or DMMP usually brings a little negative effects on the morphology and mechanical properties of FPUF, still they accorded with criterion if the adding amount was appropriate because EG or DMMP could hardly break the balance between gel reaction and blow reaction of foaming process.

In the temperature range of -80 to -50°C , 15 pbw DMMP or 15 pbw EG + 15 pbw DMMP addition made FPUF composites' storage modulus, loss modulus, the peak value of $\tan \delta$ and the

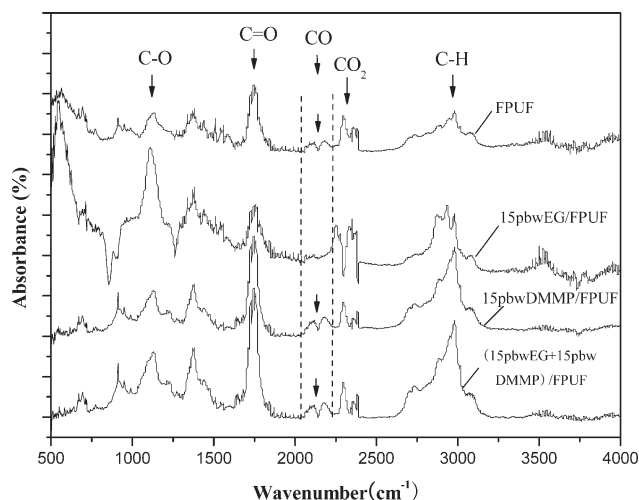


Figure 10. The FTIR spectra of gases evolved from samples as tested by TG-FTIR at 400°C.

temperature range of $\tan \delta > 0.3$ increase, indicating that they improved damping performance of FPUF due to the restriction of molecular motion by incorporation of the two additives.

The horizontal burning test results indicated that adding 10 pbw EG or 5 pbw DMMP can make FPUF achieve SE rating. According to the LOI test, there is synergistic effect between EG and DMMP and when the ratio of EG to DMMP was 1 : 2, the value of LOI reached maximum. The synergism of EG and DMMP may be caused by the formation of the stable and dense char protection layer resulting from bond force between expanded graphite layers because of viscous products from DMMP decomposition. The droplet of FPUF and DMMP/FPUF was very serious during combustion. The volume of expanded graphite covered with small crack was so large that it could inhibit droplet.

The thermal degradation of FPUF involves two steps. The first step corresponds to the degradation of the HSSs. The second step corresponds to the SSs degradation. DMMP made the first thermal degradation rate decrease while EG did not appear this case. Adding EG or DMMP decreased the second thermal degradation rate, because expanded carbon layer of EG acted as a heat insulator and DMMP dehydrated to coke residue and the products covered FPUF substrate. With the mixture of EG and DMMP added into FPUF, there is no synergistic effect for thermal stability maybe due to phosphoric acid covered large expanded graphite instead of hot-melt FPUF. Adding EG decreased the yield of CO and increased the yield of CO₂ at the

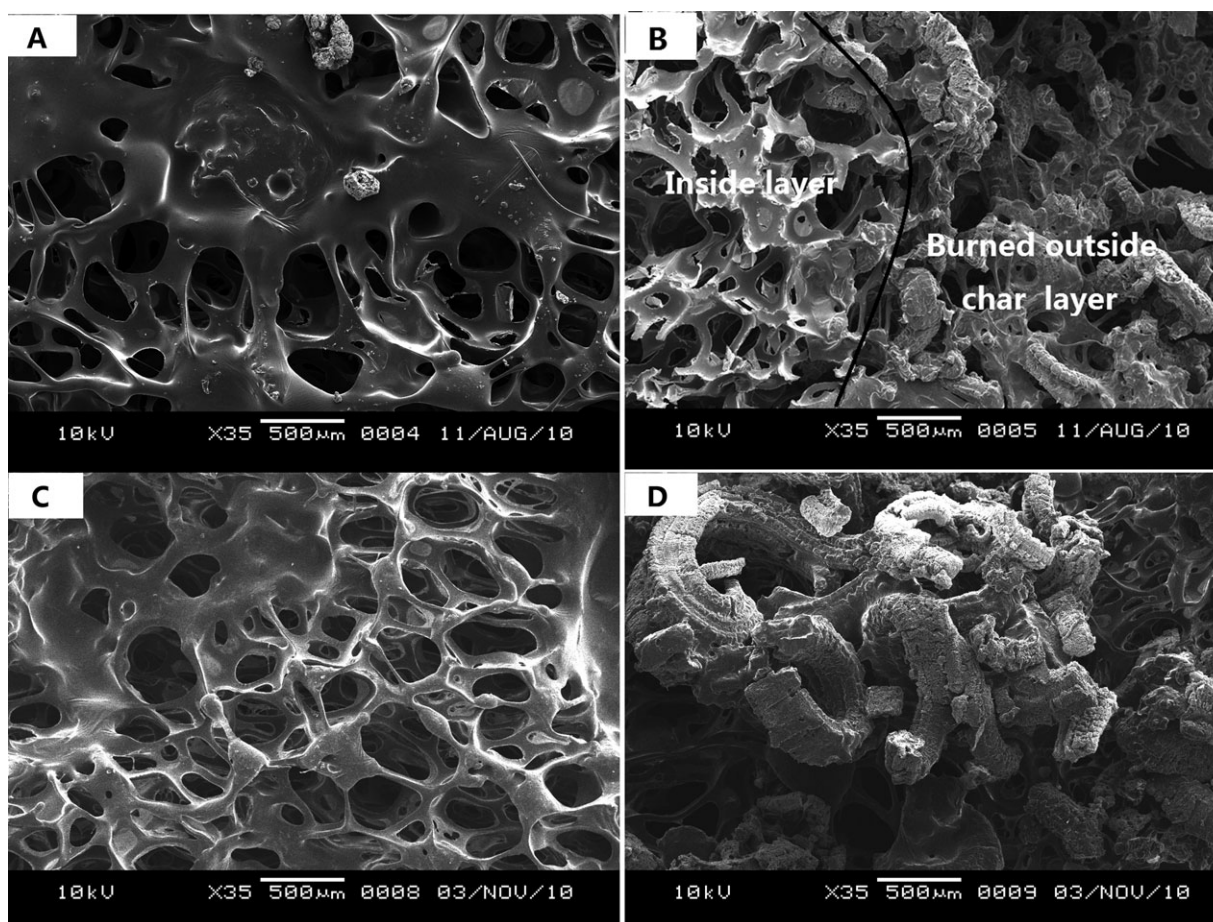


Figure 11. SEM micrographs of burned flame retardants filled FPUF. (A) FPUF (×35); (B) 15 pbw EG/FPUF (×35); (C) 15 pbw DMMP/FPUF (×35); (D) (15 pbw EG + 15 pbw DMMP)/FPUF (×35).

time of maximum decompose velocity, but DMMP increased the CO yield a little, and during the whole degradation process, DMMP increased many gases' yield due to the complicated chemical actions of DMMP on pyrolysis process of the foam.

REFERENCES

1. Labidi, S.; Azema, N.; Perrin, D.; Lopez-Cuesta, J-M. *Polym. Degrad. Stab.* **2010**, *95*, 382.
2. Dasari, A.; Yu Z. Z.; Mai Y. W.; Cai G.; Song, H. *Polymer* **2009**, *50*, 1577.
3. Chattopadhyay, D. K.; Webster, D. C. *Prog. Polym. Sci.* **2009**, *34*, 1068.
4. Modesti, M.; Lorenzetti, A. *Polym. Degrad. Stab.* **2002**, *78*, 341.
5. Thirumal, M.; Khastgir, D.; Singha, N. K.; Manjunath, B. S.; Naik, Y. P. *J. Appl. Polym. Sci.* **2008**, *110*, 2586.
6. Ye, L.; Meng, X. Y.; Liu, X. M.; Tang, J. H.; Li, Z. M. *J. Appl. Polym. Sci.* **2009**, *111*, 2372.
7. Ye, L.; Meng, X. Y.; Ji, X.; Li, Z. M.; Tang, J. H. *Polym. Degrad. Stab.* **2009**, *94*, 971.
8. Shi, L.; Li, Z. M.; Xie, B. H.; Wang, J. H.; Tian, C. R.; Yang, M. B. *Polym. Int.* **2006**, *55*, 862.
9. Meng, X. Y.; Ye, L.; Zhang, X. G.; Tang, P. M.; Tang, J. H.; Ji, X.; Li, Z. M. *J. Appl. Polym. Sci.* **2009**, *114*, 853.
10. Bian, X. C.; Tang, J. H.; Li, Z. M. *J. Appl. Polym. Sci.* **2008**, *109*, 1935.
11. Bian, X. C.; Tang, J. H.; Li, Z. M. *J. Appl. Polym. Sci.* **2008**, *110*, 3871.
12. Bian, X. C.; Tang, J. H.; Li, Z. M.; Lu, Z. Y.; Lu, A. *J. Appl. Polym. Sci.* **2007**, *104*, 3347.
13. Bashirzadeh, R.; Gharehbaghi, A. *J. Cell. Plast.* **2010**, *46*, 129.
14. Modesti, M.; Lorenzetti, A. *Polym. Degrad. Stab.* **2002**, *78*, 167.
15. Modesti, M.; Lorenzetti, A.; Simioni, F.; Camino, G. *Polym. Degrad. Stab.* **2002**, *77*, 195.
16. Xiang, H. F.; Xu, H. Y.; Wang, Z. Z.; Chen, C. H. *J. Power Sources* **2007**, *173*, 562.
17. Chen, D. M.; Zhao, Y. P.; Yan, J. J.; Chen, L.; Dong, Z. Z.; Fu, W. G. *Adv. Mater. Res.* **2012**, *418–420*, 540.
18. Sun, F. S.; Li, Y. Q.; Tian, Y.; Xin, H. B. *Polym. Indus.* **2003**, *18*, 18. (in Chinese).
19. Kaushiva, B. D.; Wilkes, G. L. *J. Appl. Polym. Sci.* **2000**, *77*, 202.
20. Kaushiva, B. D.; McCartney, S. R.; Rossmly, G. R.; Wilkes, G. L. *Polymer* **2000**, *41*, 285.
21. Konig, A.; Kroke, E. *Polym. Adv. Technol.* **2011**, *22*, 5.
22. Xiang, H. F.; Xu, H. Y.; Wang, Z. Z.; Chen, C. H. *J. Power Sources* **2007**, *173*, 562.
23. Awad, W. H.; Wilkie, C. A. *Polymer* **2010**, *51*, 2277.
24. Duquesne, S.; Michel, L. B.; Bourbigot, S.; Delobel, R.; Camino, G.; Eling, B.; Lindsay, C.; Roels, T.; Vezin, H. *J. Appl. Polym. Sci.* **2001**, *82*, 3262.
25. Price, D.; Gao, F.; John Milnes, G.; Eling, B.; Lindsay, C. I.; Mcgrail, P.T. *Polym. Degrad. Stab.* **1999**, *64*, 403.